



Supplement of

The fate of fixed nitrogen in Santa Barbara Basin sediments during seasonal anoxia

Xuefeng Peng et al.

Correspondence to: Xuefeng Peng (xpeng@seoe.sc.edu) and David L. Valentine (valentine@ucsb.edu)

The copyright of individual parts of the supplement might differ from the article licence.

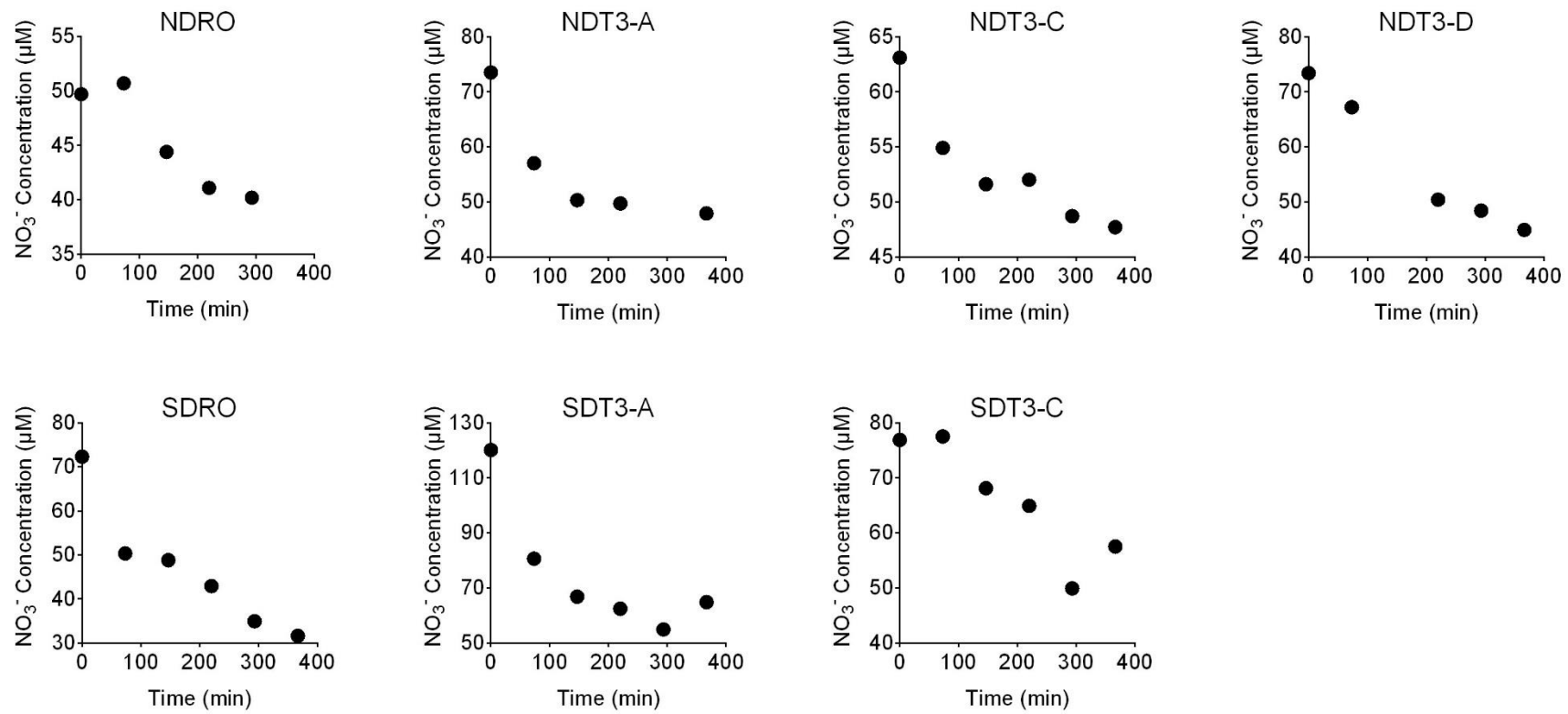


Figure S1. Nitrate (NO_3^-) concentrations in benthic flux chambers with $^{15}\text{NO}_3^-$ additions.

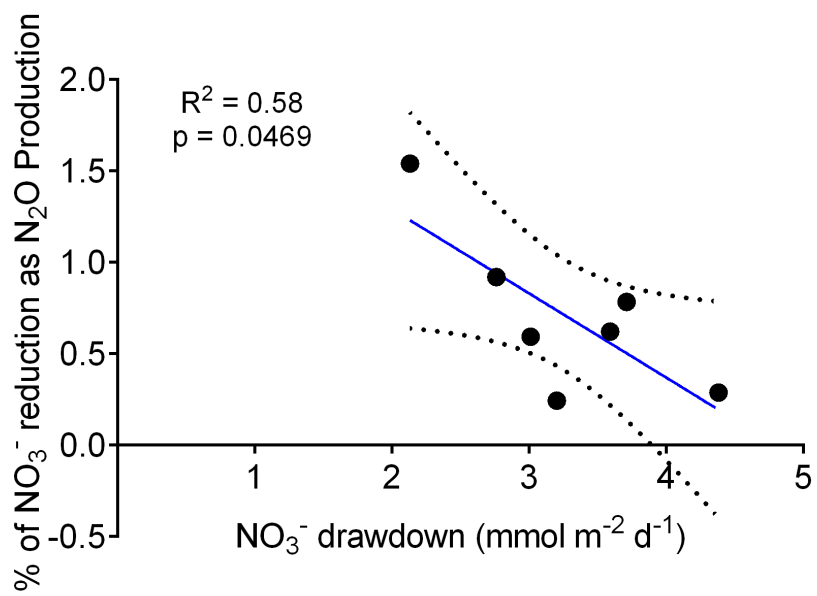


Figure S2. The correlation between NO_3^- drawdown rates measured from benthic flux chambers without $^{15}\text{NO}_3^-$ additions and the fraction of NO_3^- reduction as N_2O production. The solid line represents the best fit linear regression, and the dashed lines represent the 95% confidence interval band.

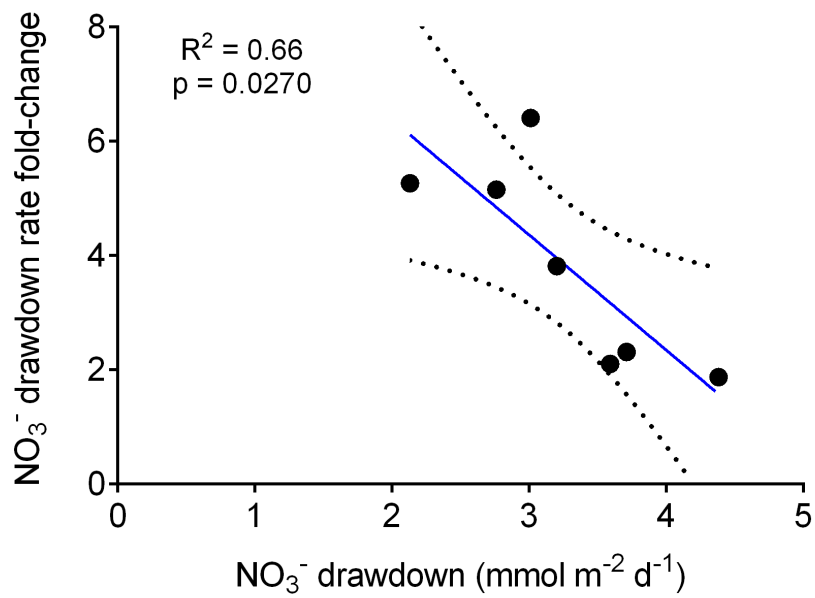


Figure S3. The correlation between NO_3^- drawdown rates measured from benthic flux chambers without $^{15}\text{NO}_3^-$ additions and the NO_3^- drawdown rate fold-change as a result of $^{15}\text{NO}_3^-$ additions (Table S2). The solid line represents the best fit linear regression, and the dashed lines represent the 95% confidence interval band.

Table S1. Detection limits of the rates of N_2 production from denitrification, N_2 production from anaerobic ammonia oxidation (anammox), NH_4^+ production from dissimilatory nitrate reduction to ammonia (DNRA), and N_2O production.

Station	NDT3-D	NDT3-C	NDT3-A	NDRO	SDRO	SDT3-A	SDT3-C
N_2 production - denitrification (mmol $\text{m}^{-2} \text{d}^{-1}$)	0.053	0.174	0.092	0.156	0.200	0.042	0.051
N_2 production - anammox (mmol $\text{m}^{-2} \text{d}^{-1}$)	0.027	0.083	0.032	0.238	0.202	0.033	0.041
NH_4^+ production from DNRA (mmol $\text{m}^{-2} \text{d}^{-1}$)	0.006	0.022	0.026	0.018	0.071	0.010	0.029
N_2O production ($\mu\text{mol m}^{-2} \text{d}^{-1}$)	2.46	1.46	1.11	1.25	5.60	3.94	2.94

Table S2. The degree of $^{15}\text{NO}_3^-$ enrichment, the fold change in bottom water NO_3^- concentration as a result of $^{15}\text{NO}_3^-$ addition; areal rates of NO_3^- drawdown with and without $^{15}\text{NO}_3^-$ addition and the calculated fold change.

Station	NDT3-D	NDT3-C	NDT3-A	NDRO	SDRO	SDT3-A	SDT3-C
% of $^{15}\text{NO}_3^-$	67%	62%	66%	73%	86%	77%	70%
NO_3^- fold change	1.99	1.62	1.90	2.75	6.17	3.43	2.30
NO_3^- drawdown rate <u>without</u> $^{15}\text{NO}_3^-$ addition (mmol m $^{-2}$ d $^{-1}$)	2.76	4.38	3.20	3.59	3.71	3.01	2.13
NO_3^- drawdown rate <u>with</u> $^{15}\text{NO}_3^-$ addition (mmol m $^{-2}$ d $^{-1}$)	14.22	8.19	12.21	7.53	8.58	19.26	11.22
NO_3^- drawdown rate fold change	5.15	1.87	3.81	2.10	2.31	6.40	5.26

Table S3. The contribution to $^{30}\text{N}_2$ production by coupled DNRA-anammox.

Station	NDT3-D	NDT3-C	NDT3-A	NDRO	SDRO	SDT3-A	SDT3-C
Contribution (%)	2.0%	1.9%	0.8%	1.5%	1.4%	0.9%	1.7%

Table S4. Bottom water nitrous oxide (N_2O) concentration and saturation at the beginning (T_0) of in-situ incubations. The saturation concentration of N_2O (12.16 nM) was calculated using the solubility equation from Weiss and Price (1980).

Station	NDT3-D	NDT3-C	NDT3-A	NDRO	SDRO	SDT3-A	SDT3-C
N_2O concentration (nM)	19.1	13.6	11.7	1.5	1.2	18.2	13.0
N_2O saturation	157%	112%	96%	12%	9%	150%	107%